Nonequilibrium indicator for the onset of epileptic seizure

Feng Zhang
State Key Laboratory of Electroanalytical Chemistry, Changchun Institute of Applied Chemistry, Chinese Academy of Sciences, Changchun, Jilin 130022, China

Jin Wang*
Department of Chemistry and Physics, State University of New York at Stony Brook, Stony Brook, New York 11794-3400, USA

(Received 19 March 2023; accepted 17 August 2023; published 6 October 2023)

The occurrence of spontaneous bursts of uncontrolled electrical activity between neurons can disrupt normal brain function and lead to epileptic seizures. Despite extensive research, the mechanisms underlying seizure onset remain unclear. This study investigates the onset of seizures from the perspective of nonequilibrium statistical physics. By analyzing the probability flux within the framework of the nonequilibrium potential-flux landscape, we establish a connection between seizure dynamics and nonequilibrium. Our findings demonstrate that the degree of nonequilibrium is sensitive to the onset of epileptic seizures. This result offers an alternative perspective on assessing seizure onset in epilepsy.

DOI: 10.1103/PhysRevE.108.044111

I. INTRODUCTION

Epilepsy is a neurological disorder characterized by spontaneous seizures, which result from a burst of uncontrolled electrical activity between neurons [1]. The abnormal synchronization of neuronal activities leads to a disturbance in brain function, making it essential to detect seizures before they cause severe symptoms. The electroencephalogram is a valuable tool that uses electrodes to measure and record brain electrical activity. Most seizure detection methods rely on monitoring electroencephalographic readings [2,3]. Abnormal electrical discharges with specific characteristic patterns can be observed during epileptic seizures.

The mechanism of the seizure generation is unclear so far due to the complexity of the brain. In the investigation of epilepsy, the researchers often regard the seizure onset as a bifurcation from the perspective of a dynamical system [4–6]. The bifurcation occurs when the dynamical structure changes; for instance, the transition from stable state to limit cycle or chaos [7]. It is often accompanied by a sudden change in the behavior of a dynamical system. The normal phase of the brain can be thought of as a stable state, while the seizure corresponds to a limit cycle or chaos. This inference is easy to capture from the brain electrical activities. The seizure burst can be detected by electroencephalography with high-amplitude pathological oscillations [2]. In contrast, the normal brain operates with low-amplitude electrical activities with a silent mode distinct from the seizure. The transition from the normal to the seizure phase can be thought of as a bifurcation from the perspective of a dynamical system. In other words, the sudden change in the bifurcation is responsible for the seizure burst in the neuronal system.

An alternative insight to understand such a transition can come from the perspective of nonequilibrium statistical physics. The seizure occurs with high-amplitude turbulent oscillations in the brain activities. In comparison, the normal brain maintains a silent mode with low-amplitude electrical activity. A similar transition from silent to turbulent activity can be found in various fields. For instance, a fluid flow imposed by temperature differences exhibits a similar behavior called Rayleigh-Bénard convection [8]. The convection flow ceases without a vertical temperature gradient. A turbulence convection arises with the development of the convective instability when the temperature difference increases over a certain threshold [9]. In addition, the laminar flow develops into a turbulence with a similar transition [10]. The Belousov-Zhabotinsky reaction system is another well-known example discovered in chemistry [11,12]. The color of the reaction solution oscillates with the concentrations of reactant species. A distinct oscillation in the solution color occurs far from equilibrium state. In contrast, the oscillation disappears near the equilibrium. Apparently, such systems undergo a transition from a silent to a turbulent activity, while the systems enter into nonequilibrium. In other words, the systems maintain a silent activity near equilibrium, and the nonequilibrium stimulates the turbulent activity.

Many systems exhibit similar nonequilibrium thermodynamic structures, despite their differences. This observation has led to an approach in understanding the underlying mechanism of epileptic seizures, which differs from conventional treatments. Due to the complexity of the brain, constructing an explicit model of the brain is challenging. However, the perspective of nonequilibrium statistical physics can offer implicit insights beyond the intricate details of the system. In this study, we aim to use this approach to understand the mechanism of seizure bursts.

II. POTENTIAL-FLUX LANDSCAPE APPROACH

A real system is inevitably influenced by the effect of noise coming from the environment or the internal microscopic

*jin.wang.1@stonybrook.edu

processes. So, a general dynamics can be described by the stochastic dynamics,

$$d\mathbf{x} = \mathbf{F}dt + d\mathbf{w}, \tag{1}$$

with the deterministic driving force $\mathbf{F}$ and the noise $d\mathbf{w}$. It is necessary to introduce a statistical description for such stochastic systems. For the continuous dynamical system, the statistical behavior is dominated by the probability density distribution $P(\mathbf{x}, t)$. The temporal evolution of the probability density is determined by the Fokker-Planck equation [13,14]

$$\frac{\partial P}{\partial t} = -\sum_i \frac{\partial J_i}{\partial x_i}, \tag{2}$$

with the probability flow in the state space

$$J_i = F_i P - \sum_j \frac{1}{2dt} \frac{\partial \langle dw_i dw_j \rangle P}{\partial x_j}. \tag{3}$$

For the noise components, the statistical average vanishes, $\langle d\mathbf{w} \rangle = 0$, and its characteristics are described by the diffusion matrix $\langle dw_i dw_j \rangle / 2dt$ for the correlations between the ith and jth components. In the steady state $\partial P_{\rm ss}/\partial t = 0$, the probability flux possesses a rotational property with divergence-free

$$\nabla \cdot \mathbf{J}^{\rm ss} = 0. \tag{4}$$

The noise correlation matrix can be separated into the form of the strength ϵ and a measure for the anisotropy of the noise

$$\langle d\mathbf{w} d\mathbf{w}^{\rm T} \rangle / 2dt = \epsilon \mathbf{D}. \tag{5}$$

A system is in equilibrium when the divergence-free steady-state probability flux vanishes. In this case, the detailed balance is maintained. But, the net steady-state probability flux leads to the breakdown of the detailed balance in the state space. Thus, the nonzero steady-state probability flux will drive a system to enter into the nonequilibrium state. The detailed balance breaking is accompanied by the entropy production with the rate. It is easy to obtain this expression of the entropy production rate from the Fokker-Planck equation.

In the zero-noise limit $\epsilon \to 0$, the steady-state probability distribution can be expanded into a Wentzel-Kramers-Brillouin series [15]:.

$$P_{\rm ss} = \frac{1}{N} \exp\left(\sum_{k=0}^{\infty} \epsilon^{k-1} \phi_k \right), \tag{6}$$

where N is a normalizing constant. The leading-order function ϕ_0 can be written as the form in the zero-noise limit

$$\phi_0 = \epsilon \ln P_{\rm ss}. \tag{7}$$

We call it the intrinsic potential function or landscape. Accordingly, the steady-state probability flux can be transformed into the intrinsic flux velocity

$$\mathbf{V} = (\mathbf{J}^{\rm ss}/P_{\rm ss})_{\epsilon \to 0}. \tag{8}$$

The steady-state Fokker-Planck equation can be rewritten in terms of the intrinsic potential in the form of the Hamilton-Jacobi equation

$$\mathbf{F} \cdot \nabla \phi_0 + \nabla \phi_0 \cdot \mathbf{D} \cdot \nabla \phi_0 = 0. \tag{9}$$

As a consequence, the intrinsic potential landscape as a Lyapunov function decreases monotonically along the deterministic dynamics [15,16]

$$\mathbf{F} \cdot \nabla \phi_0 = -\nabla \phi_0 \cdot \mathbf{D} \cdot \nabla \phi_0 \leqslant 0. \tag{10}$$

The system states evolve finally into the ground states in which the gradient of the intrinsic potential vanishes:

$$\nabla \phi_0 = 0. \tag{11}$$

In the potential-flux landscape approach [17], the deterministic driving force can be written by means of the intrinsic potential landscape and flux:

$$\mathbf{F} = -\mathbf{D} \cdot \nabla \phi_0 + \mathbf{V}. \tag{12}$$

The gradient of the intrinsic potential and the intrinsic flux velocity are perpendicular to each other [16]:

$$\mathbf{V} \cdot \nabla \phi_0 = 0. \tag{13}$$

An equilibrium system is dominated by the negative gradient of the potential function

$$\mathbf{F} = -\mathbf{D} \cdot \nabla \phi_0, \tag{14}$$

which drives the system state into the basin of the potential landscape. The system evolution ceases when the potential landscape gradient vanishes, $\nabla \phi = 0$. In contrast, the intrinsic flux is an important dynamical component for a nonequilibrium system [16,18]. The nonequilibrium system is dominated by two different components:

$$\mathbf{F} = -\mathbf{D} \cdot \nabla \phi_0 + \mathbf{V}, \tag{15}$$

i.e., the gradient of the intrinsic potential landscape and the intrinsic flux. The intrinsic flux inherits the rotational nature of the probability flux from the divergence-free condition $\nabla \cdot \mathbf{J}_{\rm ss} = 0$. Thus, the trajectories of a nonequilibrium system are often curve shaped by the intrinsic flux. The oscillation behavior in system evolution is dominated by the intrinsic flux. In other words, the oscillation cannot occur in a potential landscape gradient dominated equilibrium system. In contrast, the stable states are mainly governed by the potential landscape gradient.

The degree of nonequilibrium can be measured by the entropy production. The entropy is defined as the form

$$S = \int P \ln P d\mathbf{x}, \tag{16}$$

and its time derivative reads

$$\frac{dS}{dt} = \int \ln P \frac{\partial P}{\partial t} d\mathbf{x} = \int \ln P \nabla \cdot \mathbf{J} \, d\mathbf{x} \tag{17}$$

by inserting the Fokker-Planck equation. This expression can also be transformed into the form by integration by parts:

$$\begin{aligned} \frac{dS}{dt} &= -\int \mathbf{J} \cdot \nabla \ln P d\mathbf{x} = -\int P^{-1} \mathbf{J} \cdot \nabla P d\mathbf{x} \\ &= -\int P^{-1} \mathbf{J} \cdot (\epsilon \mathbf{D})^{-1} \cdot [(\mathbf{F} - \epsilon \nabla \cdot \mathbf{D}) P - \mathbf{J}] d\mathbf{x} \\ &= -\epsilon^{-1} \int \mathbf{J} \cdot \mathbf{D}^{-1} \cdot (\mathbf{F} - \epsilon \nabla \cdot \mathbf{D}) d\mathbf{x} \\ &\quad + \epsilon^{-1} \int P^{-1} \mathbf{J} \cdot \mathbf{D}^{-1} \cdot \mathbf{J} d\mathbf{x}. \end{aligned} \tag{18}$$

The first term has the physical meaning of the entropy change rate of the environments. Note that dS/dt stands for the entropy change in the system. Thus, the second term describes the total entropy change rate of the system and the environment. In addition, the second term is always nonnegative. Therefore, it is identified as the entropy production rate [19–21]:

$$\mathrm{EPR} = \epsilon^{-1} \int P_{\mathrm{ss}}^{-1} \mathbf{J} \cdot \mathbf{D}^{-1} \cdot \mathbf{J} d\mathbf{x} \geqslant 0. \tag{19}$$

This is the second law of thermodynamics for nonequilibrium systems. In the zero-noise limit, the steady-state probability flux can be accordingly transformed into the intrinsic flux velocity. Then, a rescaled entropy production rate can be introduced in the form of the intrinsic flux

$$\mathrm{epr} = \int \mathbf{V} \cdot \mathbf{D}^{-1} \cdot \mathbf{V} P_{\mathrm{ss}}(\mathbf{x}) d\mathbf{x} \geqslant 0. \tag{20}$$

Note that this expression is rescaled by the noise strength ϵ to grasp the primary part from the nonequilibrium intrinsic flux.

III. BREAKING OF THE TIME-REVERSAL SYMMETRY

There are two approaches when it comes to exploring a dynamical system. The first method involves analyzing the system's dynamics by developing mathematical equations that accurately model its behavior. However, this approach can be challenging, especially for complex systems, since obtaining a reliable model is often very difficult. In cases where a good model is unavailable, the second method comes into the play. This approach focuses on capturing the nonequilibrium behavior of the system using a data analysis method. Specifically, it involves examining the difference in the cross correlations of the time series data both forward and backward in time as a quantitative measure of nonequilibrium [22]. It provides a practical alternative, allowing us to extract meaningful information such as the degree of nonequilibrium from the available data without relying on a detailed mathematical description.

The fluctuation of a feature $A[\mathbf{x}(t+\tau)]$ may be influenced by another feature $B[\mathbf{x}(t)]$. Then, the correlation function is introduced to describe the dependence of both variables in time. In the steady state, the correlation function is dependent only on the time distance τ. The correlation function can be defined as the form [13]

$$\begin{aligned} K_{AB}(\tau) &= \langle A(t+\tau) B(t) \rangle \\ &= \int A(\mathbf{x}) B(\mathbf{x}') w(\mathbf{x}, t+\tau | \mathbf{x}', t) P_{\mathrm{ss}}(\mathbf{x}') d\mathbf{x} d\mathbf{x}', \end{aligned} \tag{21}$$

where the transition probability density $w(\mathbf{x}, t+\tau|\mathbf{x}', t)$ stands for the probability density of transition from state $\mathbf{x}'$ to state $\mathbf{x}$ in a period τ of time.

The transition probability density possesses the form of the Fokker-Planck equation [13]

$$w(\mathbf{x}, t+\tau|\mathbf{x}', t) = e^{\tau L_{\mathrm{FP}}} \delta(\mathbf{x} - \mathbf{x}') \tag{22}$$

with the Fokker-Planck operator

$$L_{\mathrm{FP}} = -\sum_i \frac{\partial}{\partial x_i} F_i + \sum_{ij} \frac{\partial^2}{\partial x_i \partial x_j} \frac{\langle dw_i dw_j \rangle}{2dt}. \tag{23}$$

Then, the correlation function can be written as the form

$$K_{AB} = \int A(\mathbf{x}) e^{\tau L_{\mathrm{FP}}} B(\mathbf{x}) P_{\mathrm{ss}}(\mathbf{x}) d\mathbf{x}, \tag{24}$$

and further, its change rate with respect to the time delay reads

$$\frac{\partial K_{Ax_k}}{\partial \tau} = \int A(\mathbf{x}) e^{\tau L_{\mathrm{FP}}} L_{\mathrm{FP}} x_k P_{\mathrm{ss}}(\mathbf{x}) d\mathbf{x}, \tag{25}$$

where we take the second variable as $B = x_k$. The operation associated with the Fokker-Planck operator can be simplified into the form

$$\begin{aligned} L_{\mathrm{FP}} x_k P_{\mathrm{ss}} &= -\sum_i \frac{\partial F_i x_k P_{\mathrm{ss}}}{\partial x_i} + \frac{1}{2dt} \sum_{ij} \frac{\partial^2 \langle dw_i dw_j \rangle x_k P_{\mathrm{ss}}}{\partial x_i \partial x_j} \\ &= -x_k \sum_i \frac{\partial F_i P_{\mathrm{ss}}}{\partial x_i} - \sum_i \frac{\partial x_k}{\partial x_i} F_i P_{\mathrm{ss}} \\ &\quad + \frac{1}{2dt} \sum_{ij} \frac{\partial \langle dw_i dw_j \rangle P_{\mathrm{ss}}}{\partial x_i} \frac{\partial x_k}{\partial x_j} \\ &\quad + \frac{1}{2dt} \sum_{ij} \left[\frac{\partial x_k}{\partial x_i} \frac{\partial \langle dw_i dw_j \rangle P_{\mathrm{ss}}}{\partial x_j} \right. \\ &\quad \left. + x_k \frac{\partial^2 \langle dw_i dw_j \rangle P_{\mathrm{ss}}}{\partial x_i \partial x_j} \right] \\ &= -x_k L_{\mathrm{FP}} P_{\mathrm{ss}} - F_k P_{\mathrm{ss}} + 2 \sum_j \frac{1}{2dt} \frac{\partial \langle dw_k dw_j \rangle P_{\mathrm{ss}}}{\partial x_j} \\ &= -F_k P_{\mathrm{ss}} + 2 \sum_j \frac{1}{2dt} \frac{\partial \langle dw_k dw_j \rangle P_{\mathrm{ss}}}{\partial x_j}, \end{aligned} \tag{26}$$

where the steady state induces $L_{\mathrm{FP}} P_{\mathrm{ss}} = 0$ in the last step. In addition, we can further obtain an expression associated with the probability flow from Eq. (3):

$$L_{\mathrm{FP}} x_k P_{\mathrm{ss}} = \sum_j \frac{1}{2dt} \frac{\partial \langle dw_k dw_j \rangle P_{\mathrm{ss}}}{\partial x_j} - J_k^{\mathrm{ss}}. \tag{27}$$

Therefore, the change rate of the correlation function of x_i and x_j can be further written as the form

$$\begin{aligned} \left. \frac{\partial K_{x_i x_j}}{\partial \tau} \right|_{\tau=0} &= \int x_i \left[\sum_l \frac{1}{2dt} \frac{\partial \langle dw_j dw_l \rangle P_{\mathrm{ss}}}{\partial x_l} - J_j^{\mathrm{ss}} \right] d\mathbf{x} \\ &= \int \left[-\frac{\langle dw_j dw_i \rangle}{2dt} P_{\mathrm{ss}} - x_i J_j^{\mathrm{ss}} \right] d\mathbf{x} \\ &= -\frac{\langle\langle dw_j dw_i \rangle\rangle}{2dt} - \int x_i J_j^{\mathrm{ss}} d\mathbf{x}, \end{aligned} \tag{28}$$

where the second equality is obtained by integration by parts and natural boundary condition. A difference in the cross-correlation forward (i.e., $\langle x_i(t+\tau) x_j(t) \rangle$) and backward (i.e., $\langle x_i(t-\tau) x_j(t) \rangle$) in time arises due to the probability flow

$$\left. \frac{\partial K_{x_i x_j} - K_{x_j x_i}}{\partial \tau} \right|_{\tau=0} = \int \left(x_j J_i^{\mathrm{ss}} - x_i J_j^{\mathrm{ss}} \right) d\mathbf{x}. \tag{29}$$

Here, note that the backward term is written in the form $\langle x_i(t-\tau) x_j(t) \rangle = \langle x_i(t) x_j(t+\tau) \rangle = K_{x_j x_i}$. In addition, we

can establish such a relation about the probability flow

$$\begin{aligned}\int \sum_k \frac{\partial x_i x_j J_k^{ss}}{\partial x_k} d\mathbf{x} &= 0 \\ &= \int x_j J_i^{ss} d\mathbf{x} + \int x_i J_j^{ss} d\mathbf{x} + \int x_i x_j \sum_k \frac{\partial J_k^{ss}}{\partial x_k} d\mathbf{x} \\ &= \int \left(x_j J_i^{ss} + x_i J_j^{ss}\right) d\mathbf{x} \end{aligned} \tag{30}$$

where the last equality is due to the nature of divergence-free of the probability flow. Therefore, the difference in correlation forward and backward in time can be simplified as the form

$$\left.\frac{\partial\left(K_{x_i x_j} - K_{x_j x_i}\right)}{\partial \tau}\right|_{\tau=0} = 2\int x_j J_i^{ss} d\mathbf{x} = -2\int x_i J_j^{ss} d\mathbf{x}. \tag{31}$$

The time reversal symmetry is conserved in the equilibrium systems due to the detailed balance $\mathbf{J} = 0$. In contrast, in the nonequilibrium systems, the probability flow gives rise to the asymmetry between the cross correlation functions $\langle x_i(t+\tau)x_j(t)\rangle$ and $\langle x_i(t-\tau)x_j(t)\rangle$.

IV. SEIZURE DYNAMICS

An epilepsy model was proposed to characterize the onset as a saddle-node bifurcation and offset as homoclinic bifurcation [6,23]. This model consists of two subsystems with two types of variables by x standing for the membrane potential and y relating to the ions current [6,23]. The first subsystem with two state variables x_1 and y_1 is responsible for the fast discharges. The second subsystem generates sharp-wave events described by two state variables x_2 and y_2. In addition, a slow permittivity variable z drives the seizure dynamics taking effect as a mean field of the extracellular processes [6]. The seizure dynamics reads as following equations [6,23]:

$$\dot{x}_1 = y_1 - f_1(x_1, x_2) - z + 3.1 \tag{32}$$

$$\dot{y}_1 = 1 - 5x_1^2 - y_1 \tag{33}$$

$$\dot{x}_2 = -y_2 + x_2 - x_2^3 + 0.45 + 0.002g(x_1) - 0.3(z - 3.5) \tag{34}$$

$$\dot{y}_2 = 10^{-1}(-y_2 + f_2(x_1, x_2)) \tag{35}$$

$$\dot{z} = 2857^{-1}[4(x_1 + 1.6) - z], \tag{36}$$

where the additional functions are defined in the form

$$g(x) = \int_{t_0}^{t} e^{-0.01(t-\tau)} x(\tau) d\tau, \tag{37}$$

$$f_1(x_1, x_2) = \begin{cases} x_1^3 - 3x_1^2 & \text{if } x_1 < 0 \\ [x_2 - 0.6(z-4)^2]x_1 & \text{if } x_1 \geqslant 0, \end{cases} \tag{38}$$

$$f_2(x_1, x_2) = \begin{cases} 0 & \text{if } x_2 < -0.25 \\ 6(x_2 + 0.25) & \text{if } x_2 \geqslant -0.25. \end{cases} \tag{39}$$

The first two equations for $\dot{x}_1$ and $\dot{y}_1$ describe the burst generation after a short current pulse [24]. The rudiment comes from the Van der Pol model for nonlinear relaxation oscillators in electrical circuits, and later this model is extended to the biological science such as describing the action potentials of neurons [25]. In spite of large modification, one can find some particular terms are also shared by the Van der Pol model; for instance, the cubic term x_1^3 in the first equation $\dot{x}_1$ via the function $f_1(x_1, x_2)$. The subsequent two equations for $\dot{x}_2$ and $\dot{y}_2$ reproduce the spiking behavior of neurons [26]. These two equations are based on the Morris-Lecar model describing the oscillations in relation to the Ca^{++} and K^+ conductance in barnacle muscle [27].

It is worthwhile to notice that the permittivity variable z changes quite slowly compared with other variables

$$\dot{z} \to 0. \tag{40}$$

Thus, the seizure dynamics in the original model can be modified as an adiabatic process with respect to the slow variable:

$$\dot{x}_1 = y_1 - f_1(x_1, x_2) - z + 3.1, \tag{41}$$

$$\dot{y}_1 = 1 - 5x_1^2 - y_1, \tag{42}$$

$$\dot{x}_2 = -y_2 + x_2 - x_2^3 + 0.45 + 0.002g(x_1) - 0.3(z - 3.5) \tag{43}$$

$$\dot{y}_2 = 10^{-1}[-y_2 + f_2(x_1, x_2)]. \tag{44}$$

In this case, the adiabatic slow variable z becomes a control parameter of the epilepsy model. Furthermore, an additional variable u can be introduced instead of the integral function $g(x)$ with the form $u = g(x)$. Then, the seizure dynamics of the brain system can be written in the form

$$dx_i = F_i dt + dw_i, \tag{45}$$

with the deterministic driving force

$$F_1 = x_2 - f_1(x_1, x_3) - z + 3.1, \tag{46}$$

$$F_2 = 1 - 5x_1^2 - x_2, \tag{47}$$

$$F_3 = -x_4 + x_3 - x_3^3 + 0.45 + 0.002x_5 - 0.3(z - 3.5), \tag{48}$$

$$F_4 = 10^{-1}[-x_4 + f_2(x_1, x_3)], \tag{49}$$

$$F_5 = -0.01x_5 + x_1, \tag{50}$$

and we add some noises to the system dynamics

$$\langle dw_i dw_j\rangle/2dt = 0.001\delta_{ij}. \tag{51}$$

Note that the variable names are replaced as a unified form x_i for concise expression.

The seizure dynamics can be captured by the trajectories in the state space as given by Figs. 1(a)–1(d). There are two different phases: the normal phase represented by blue color and the seizure phase by red trajectory. The normal phase is in a stable state, while the seizure phase exhibits a chaotic oscillation. The system is in the seizure phase in the regime of small permittivity z with a chaotic oscillation [Fig. 1(a)]. As the permittivity increases, a normal phase appears and coexists with the seizure phase [Figs. 1(b) and 1(c)]. As the permittivity increases further, the seizure phase disappears and the system is dominated by the normal phase [Fig. 1(d)].

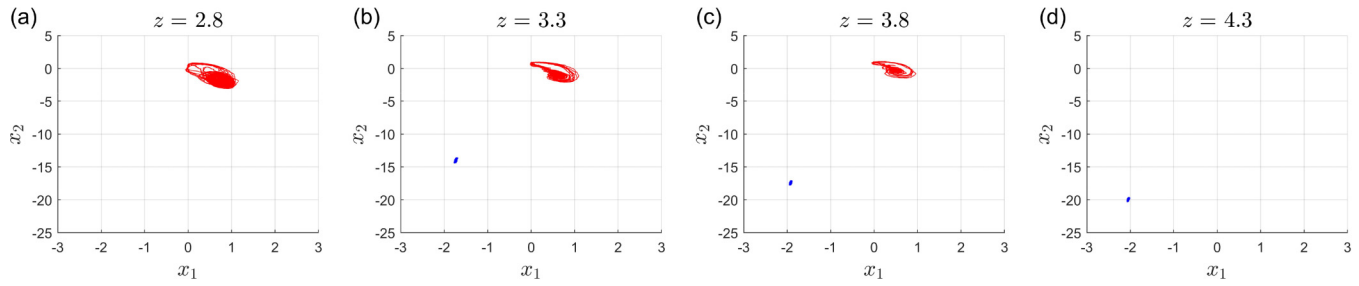

FIG. 1. Stochastic trajectories with different permittivity parameters. (a) The seizure phase is stable with a chaotic oscillating trajectory under low permittivity. (b),(c) The normal phase arises with the form of stable state upon increasing the permittivity parameter. The normal and seizure phases coexist in this case. (d) The normal phase dominates the brain system under high permittivity, while the seizure phase disappears.

A continuous change with the transition between different phases is given by Fig. 2. The average state of $\bar{x}_2$ is employed to characterize different phases (normal or seizure). The upper branch with red asterisks stands for the seizure phase, and the lower branch with blue circles corresponds to the normal phase. In practical calculations, we obtain first the trajectory from the dynamical equations, and take the trajectory average for the average state of $\bar{x}_2$. It is easy to see the transitions between normal and seizure phases from Fig. 2. At low permittivity, the seizure phase is more stable than the normal phase, and thus the system tends to stay in the seizure phase. In contrast, the normal phase gradually becomes stable as the permittivity increases. Two phase branches coexist in the parameter regime roughly $2.95 \leqslant z \leqslant 3.95$. At high permittivity, the seizure phase is unstable, and the system enters into the normal phase. We can see a path-dependent evolution or hysteresis of the system. The transition from normal to seizure phase occurs near $z = 2.95$ as the permittivity parameter decreases. In contrast, when the parameter increases, the transition from seizure to normal phase occurs near $z = 3.95$. At the transition points, a tiny change of the parameter can cause a large shift of the system state between different branches.

This study aims to examine the changes in system behavior. These changes can also be analyzed using bifurcation theory [28], which is a more mathematical approach and attributes the changes to explicit modifications in the structure of the dynamical equations, such as adjusting a specific parameter. In contrast, the potential-flux approach offers a more physical explanation of the changes. It suggests that the degree of nonequilibrium in the system is what leads to the alterations in behavior. The advantage of our potential-flux approach lies in its ability to understand and grasp the nonequilibrium origin of these changes.

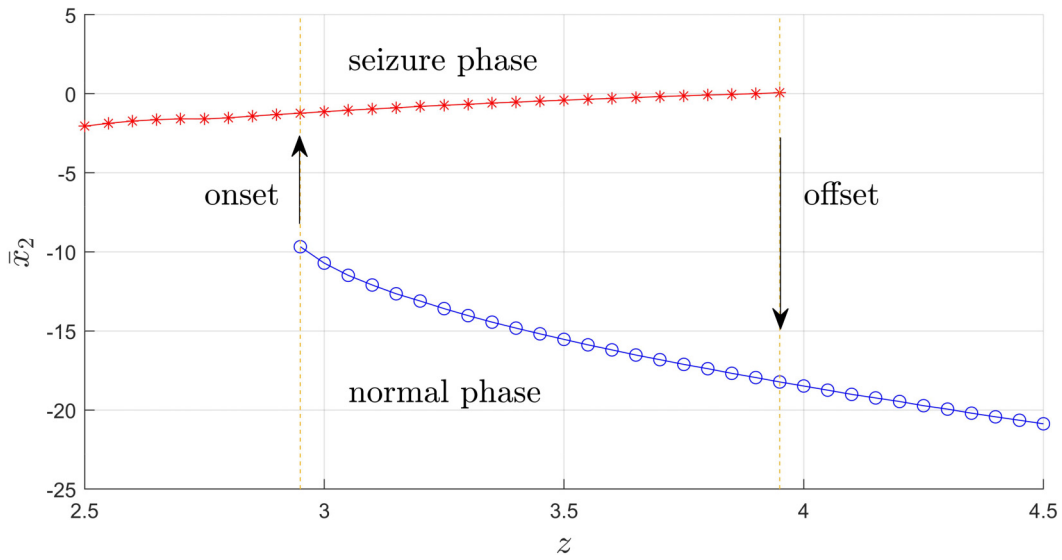

FIG. 2. Transition between the normal and seizure phases. The upper branch with red asterisks stands for the seizure phase, and the lower branch with blue circles corresponds to the normal phase. At high permittivity, the system has a stable normal phase and unstable seizure phase. Thus, the system stays in the normal phase. Two branches coexist as the permittivity decreases. The system enters into one of two phases. At low permittivity, the seizure phase is more stable than the normal phase and thus the seizure occurs. At the transition points, a tiny change of the parameter can cause a large shift of the system state between different branches. The onset of seizure occurs at the permittivity parameter near threshold value $z \sim 3$.

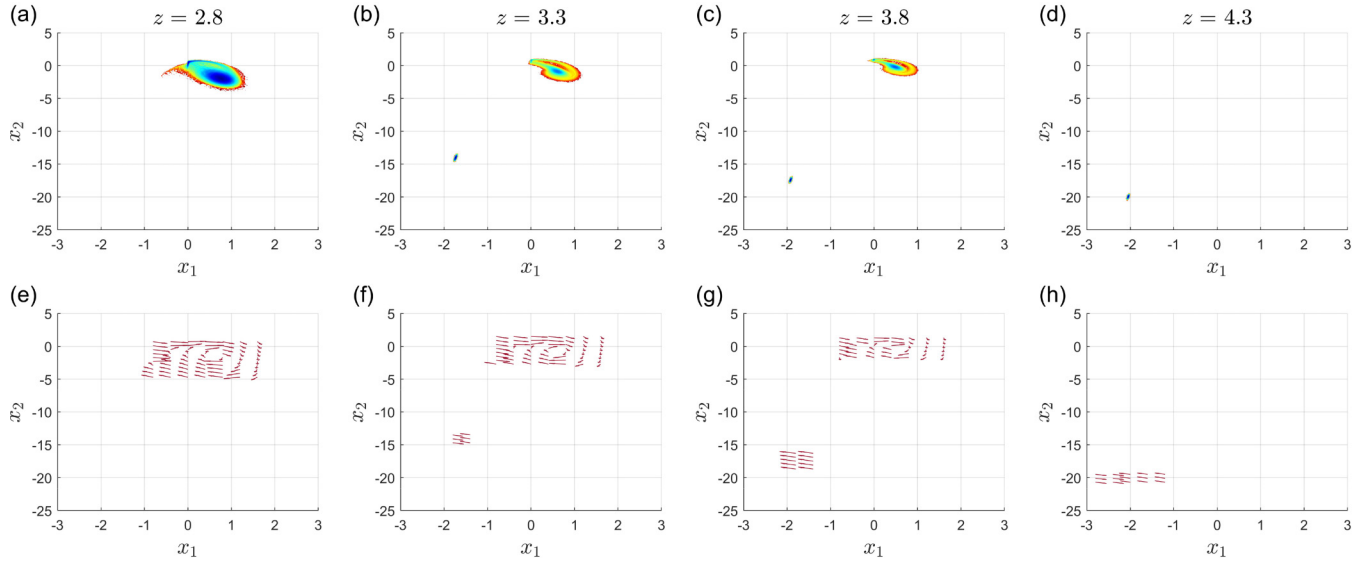

FIG. 3. An illustration of potential and flux for qualitative discussion. (a)–(d) Potential function. The blue stands for the low potential and red corresponds to the high potential. The system tends to evolve into the bluest states by the effect of the negative potential gradient. (e)–(h) Probability flux. The flux exhibits rotation due to the divergence-free nature. The trajectories attracted toward ground states are curved by the probability flux.

V. ONSET OF SEIZURE ASSOCIATED WITH NONEQUILIBRIUM

The potential-flux landscape approach provides a perspective to capture the effect of nonequilibrium on the system dynamics [17]. Due to their dissipative nature, the system states are attracted into a basin with ground states. Figures 3(a)–3(d) illustrate the intrinsic potential landscape. The potential reduces as the color changes from red to blue, i.e., the blue stands for the low potential and red corresponds to the high potential. The bluest states are the ground states. The system evolves into the ground states by the effect of the negative potential gradient. The negative gradient of the intrinsic potential is responsible for the attraction to the basin constituted mainly by ground states. On the other hand, the trajectory is curved by the intrinsic flux as shown in Figs. 3(e)–3(h), due to the divergence-free nature of the intrinsic flux. In other words, the steady-state probability flux exhibits rotation due to the divergence-free nature. The trajectories attracted towards the ground states are curve shaped by the probability flux. The probability flux breaks the detailed balance of the system. The appearance of the intrinsic flux indicates that the system enters into the nonequilibrium state.

The epilepsy is characterized by the chaotic oscillation behavior of the brain system. As mentioned in the previous discussion, the oscillation behavior is driven by the nonequilibrium intrinsic flux. In contrast, the normal phase is a stable state mainly dominated by the potential gradient. Thus, the onset of a seizure can be thought of as a transition from quasi- or near equilibrium to nonequilibrium states. So, we can track the change of nonequilibrium degree to capture the transition from normal to seizure phases.

As mentioned previously, the system evolution is affected by the driving force component of the intrinsic flux in the case of nonequilibrium. Since the flux is rotational, it tends to destabilize the point attractor and generate rotational line states such as chaotic oscillations. This gives the dynamical origin of the phase transition from normal phase to the epileptic seizure generation. Thus, the magnitude of the intrinsic flux reflects the degree of nonequilibrium from the perspective of dynamics:

$$\kappa = \int |\mathbf{V}| P_{\rm ss} d\mathbf{x}. \tag{52}$$

Note that the second equality is due to the disappearance of the gradient of the intrinsic potential in the ground states.

The effect of the intrinsic flux, and further, the degree of nonequilibrium is hidden in the trajectories of the system evolution. As discussed previously (Sec. III), the probability flow gives rise to the asymmetry in the cross-correlation functions

$$\chi = (\sigma_i \sigma_j)^{-1} \int \left| \frac{d[x_i(0)x_j(\tau) - x_j(0)x_i(\tau)]}{d\tau} \right| P_{\rm ss} d\mathbf{x}, \tag{53}$$

where we normalize this value by the standard deviations σ_i and σ_j of the ith and jth components, respectively. The time-reversal asymmetry in the cross-correlation function χ provides a direct measure of the nonequilibrium processed from the time series of the trajectories of the system evolution.

The nonequilibrium state is accompanied by the entropy production. The entropy production rate provides the thermodynamic cost associated to such dynamical nonequilibrium transition from normal to seizure phase. Therefore, the onset of seizure will be reflected in the change of entropy production rate

$$\text{epr} = \int \mathbf{V} \cdot \mathbf{D}^{-1} \cdot \mathbf{V} P_{\rm ss}(\mathbf{x}) d\mathbf{x} \geqslant 0. \tag{54}$$

Note that this expression is rescaled by the noise strength ϵ to grasp the primary part from the nonequilibrium intrinsic flux.

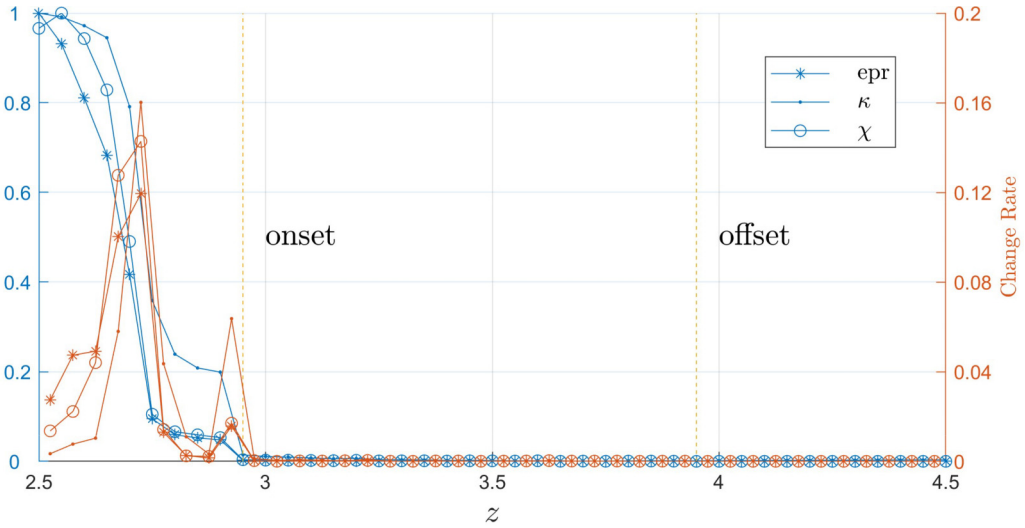

FIG. 4. Onset of seizure upon the increase in the degree of nonequilibrium. The nonequilibrium is measured from different perspectives: entropy production rate with the rescaled form epr, magnitude of the intrinsic flux κ, and time-reversal asymmetry χ. Note that these values are normalized by their respective maximums. A sudden change in the degree of nonequilibrium synchronizes with the onset of seizure as shown by the blue curves. As a reference, the orange curves show the corresponding change or the slope in the degree of nonequilibrium. It is clear that the change in the nonequilibrium degree is sensitive to the seizure onset.

On the other hand, the decreasing nature of the intrinsic potential as a Lyapunov function implies that the effective part of the intrinsic potential landscape can be retained as the form

$$\delta\phi_0 = \phi_0(\mathbf{x}) - \phi_0^{\min} \tag{55}$$

associated with the ground potential $\phi_0^{\min}$. In fact, the ground potential is the integral constant of the Hamilton-Jacobi equation, because the latter equation is constituted by the derivatives with respect to the intrinsic potential function. Therefore, the probability distribution $P_{\rm ss}$ can be written in the form of the effective part of the intrinsic potential:

$$P_{\rm ss} = \frac{1}{N}\exp\left[-\frac{\delta\phi_0}{\epsilon}\right]_{\epsilon\to 0}. \tag{56}$$

Apparently, the occurrence of the deviation from the ground states $\phi_0(\mathbf{x}) - \phi_0^{\min} \gg \epsilon$ is impossible because the probability decays sharply, as the noise strength decreases, $\epsilon \to 0$. This implies that the system state stays in the ground states with the minimum intrinsic potential $\phi_0^{\min}$ in the case of small noise $\epsilon \to 0$. In this case, the ground states can be thought of as the same probability density

$$P_{\rm ss} \simeq N^{-1}. \tag{57}$$

In the ground states, the potential gradient vanishes, $\nabla\phi_0 = 0$, and thus the deterministic driving force is dictated by the flux components

$$\mathbf{F} = -\mathbf{D}\cdot\nabla\phi_0 + \mathbf{V} = \mathbf{V}. \tag{58}$$

Therefore, the magnitude of the intrinsic flux can be rewritten in the form

$$\kappa = \int |\mathbf{V}|P_{\rm ss}d\mathbf{x} = \int |\mathbf{F}|P_{\rm ss}d\mathbf{x}, \tag{59}$$

and the rescaled entropy production rate reads

$$\text{epr} = \int \mathbf{F}\cdot\mathbf{D}^{-1}\cdot\mathbf{F}P_{\rm ss}d\mathbf{x}. \tag{60}$$

As a further approach, we take the temporal average instead of the statistical average:

$$\kappa = \frac{1}{T}\int_0^{T\to\infty} |\mathbf{V}|dt = \frac{1}{T}\int_0^{T\to\infty} |\mathbf{F}|dt, \tag{61}$$

$$\text{epr} = \frac{1}{T}\int_0^{T\to\infty} \mathbf{F}[\mathbf{x}(t)]\cdot\mathbf{D}^{-1}\cdot\mathbf{F}[\mathbf{x}(t)]dt. \tag{62}$$

In addition, the time-reversal asymmetry between different ith and jth components can also be written in the form of a temporal average:

$$\chi = \frac{1}{\sigma_i\sigma_j T}\int_0^{T\to\infty}\left|\frac{d[x_i(t)x_j(t+\tau) - x_j(t)x_i(t+\tau)]}{d\tau}\right|dt. \tag{63}$$

The result for the comparison of seizure onset with the increase of nonequilibrium degree is given in Fig. 4. The transition from normal to seizure phase is shown in Fig. 2. One can see a close connection between seizure onset and the increase of nonequilibrium degree by comparing Figs. 2 and 4. The magnitude of intrinsic flux as a dynamical measure for the nonequilibrium is shown in Fig. 4 by the blue dot curve with the left y axis. In addition, the time-reversal asymmetry between components x_1 and x_2 is shown in Fig. 4 by a blue circle curve. The turbulent oscillations are dissipative with large entropy production from the perspective of nonequilibrium thermodynamics. An implicit nonequilibrium condition is imposed on the system to provide sufficient thermodynamical cost in the seizure as shown in Fig. 4 by the blue asterisk curve.

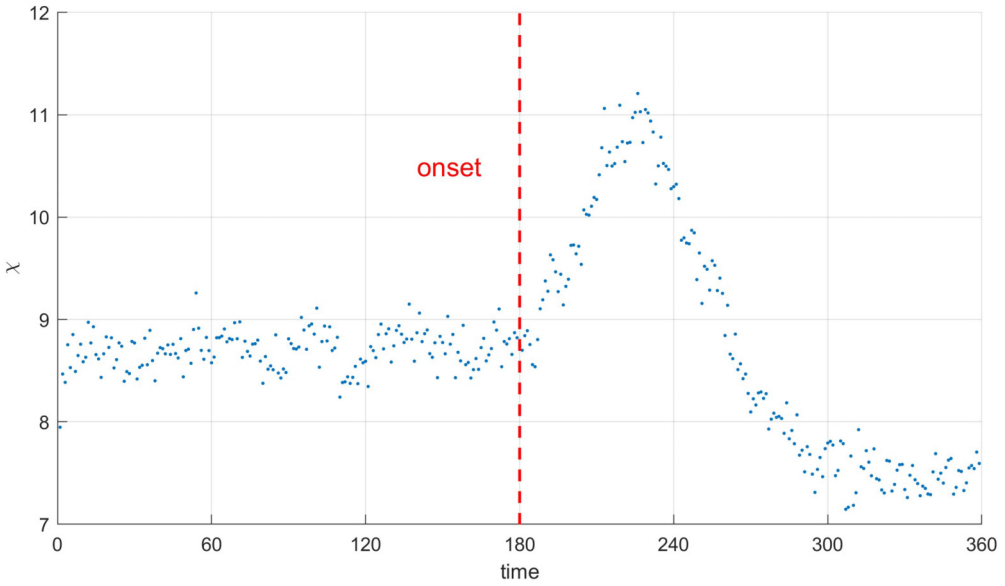

FIG. 5. The signature for the significant change in the degree of nonequilibrium as an indicator of seizure onset by using actual electroencephalographic data. The degree of nonequilibrium measured by the time-reversal asymmetry χ based on the difference in the cross correlation forward and backward in time of the electroencephalographic data.

There are various types of bifurcations. The bifurcation in a dynamical system can occur in different forms. In the seizure model employed in this study, the seizure onset results from a saddle-node bifurcation, and a homoclinic bifurcation leads to the offset [6,23]. The change strengths of the degree of nonequilibrium from different perspectives are shown in Fig. 4 by orange curves with the right y axis. One can see a distinct enhancement appears in the change strengths with the seizure burst. It is easy to see that the nonequilibrium is sensitive to the seizure onset. This result can provide an alternative indicator for the detection of the seizure bursts in epilepsy.

It is essential to assess the availability of the nonequilibrium in the assessment of the onset of seizure. Here, we utilize an electroencephalographic dataset consisting of n ($n = 100$) records from 16 patients [29]. The electroencephalographic signals in each recording are collected at a rate of 512 Hz, and the seizure onsets start at 3 min from the beginning of the recording. Figure 5 shows the availability assessment of the nonequilibrium as an indicator of the onset of seizure. The nonequilibrium measured by the time-reversal asymmetry χ is based on the difference in cross correlation of the electroencephalographic data forward and backward in time. The time series is divided into segments of 1 s duration, and the value of the time-reversal asymmetry is calculated for each segment. The dataset includes recordings from different patients with m_k ($36 \leqslant m_k \leqslant 100$) of electrodes, where $k (1 \leqslant k \leqslant n)$ stands for the sequence number of the records [29]. Thus, there are multiple pairs (ij) $(1 \leqslant i, j \leqslant m_k)$ of the cross-correlation values and their corresponding χ_{ij}^k values for each record. To measure the overall nonequilibrium, the average value of χ is computed as $\chi = \sum_{kij} |\chi_{ij}^k|/(nm_k^2)$, where the modulus operation is used because the contribution to the nonequilibrium arises from the deviation away from a zero value. In Fig. 5, a significant change in the degree of nonequilibrium can be observed near the onset of the actual seizure events. This implies that the nonequilibrium in terms of the time-reversal asymmetry χ can provide an alternative indicator of the onset of seizure.

VI. DISCUSSION AND CONCLUSION

Epilepsy is characterized by a burst of chaotic oscillation behaviors of the neuron system. The normal brain operates with low-amplitude electrical activity with a silent mode. The oscillation behavior of a dynamical system is driven by the nonequilibrium intrinsic flux, and this cannot occur in an equilibrium system. Thus, the onset of seizure can be roughly thought of as a transition from a near or quasiequilibrium state to a nonequilibrium state.

A similar phenomenon with a significant burst of chaotic oscillation can also be found in various fields. For instance, chemical reaction systems also exhibit similar dynamic behaviors when the nonequilibrium condition reaches a certain threshold value [30]. In this case, the difference in chemical potential as another type of nonequilibrium condition is responsible for the onset of chaotic oscillation in chemical systems. The increase in nonequilibrium condition results in the burst of oscillation behavior. This is easy to see from our potential-flux approach. The intrinsic flux breaks the detailed balance driving the systems into the nonequilibrium state. In addition, the intrinsic flux acts as an important dynamical component for driving the oscillation behaviors. A silent dynamical system is transitioned into a turbulent burst with the change in the nonequilibrium condition.

Our study can provide an understanding of the mechanism of the epileptic seizures from the perspective of nonequilibrium statistical physics. The change in the nonequilibrium degree can reflect the transition from the normal to the seizure phase. The change of the nonequilibrium degree can be

measured by different perspectives: the nonequilibrium driving force in terms of the magnitude of the intrinsic flux, the nonequilibrium thermodynamic cost in terms of the entropy production rate, and time-reversal asymmetry in terms of the difference between the cross correlations of time series forward and backward in time. Interestingly, they are sensitive to the seizure onset. The time-reversal asymmetry can provide an alternative indicator for the seizure burst. In addition, there is perhaps a possibility of the existence of an implicit nonequilibrium condition to trigger the seizure burst. It inspires an exploration on the further development of the seizure model.

ACKNOWLEDGMENTS

F.Z. acknowledges support from National Natural Science Foundation of China under Grant No. 21721003, and the Scientific Instrument Developing Project of the Chinese Academy of Sciences under Grant No. YJKYYQ20180038.

[1] T. R. Browne and G. L. Holmes, *Handbook of Epilepsy* (Lippincott Williams & Wilkins, Philadelphia, 2008).
[2] P. L. Nunez, *Neocortical Dynamics and Human EEG Rhythms* (Oxford University Press, New York, 1995).
[3] U. R. Acharya, S. V. Sree, G. Swapna, R. J. Martis, and J. S. Suri, Automated EEG analysis of epilepsy: A review, Knowl.-Based Syst. **45**, 147 (2013).
[4] P. Suffczynski, S. Kalitzin, and F. H. L. Da Silva, Dynamics of non-convulsive epileptic phenomena modeled by a bistable neuronal network, Neuroscience **126**, 467 (2004).
[5] M. Breakspear, J. A. Roberts, J. R. Terry, S. Rodrigues, N. Mahant, and P. A. Robinson, A unifying explanation of primary generalized seizures through nonlinear brain modeling and bifurcation analysis, Cereb. Cortex **16**, 1296 (2006).
[6] V. K. Jirsa, W. C. Stacey, P. P. Quilichini, A. I. Ivanov, and C. Bernard, On the nature of seizure dynamics, Brain **137**, 2210 (2014).
[7] P. Blanchard, R. L. Devaney, and G. R. Hall, *Differential Equations* (Brooks/Cole, Cengage Learning, Boston, MA, 2012).
[8] A. V. Getling, *Rayleigh–Bénard Convection: Structures and Dynamics* (World Scientific, Singapore, 1998).
[9] E. N. Lorenz, Deterministic nonperiodic flow, J. Atmos. Sci. **20**, 130 (1963).
[10] S. B. Pope, *Turbulent Flows* (Cambridge University Press, Cambridge, UK, 2000).
[11] R. A. Schmitz, K. R. Graziani, and J. L. Hudson, Experimental evidence of chaotic states in the Belousov–Zhabotinskii reaction, J. Chem. Phys. **67**, 3040 (1977).
[12] I. R. Epstein and J. A. Pojman, *An Introduction to Nonlinear Chemical Dynamics: Oscillations, Waves, Patterns, and Chaos* (Oxford University Press, New York, 1998).
[13] M. Risken, *The Fokker–Planck Equation: Methods of Solution and Applications* (Springer, New York, 1989).
[14] C. W. Gardiner, *Handbook of Stochastic Methods: For Physics, Chemistry and the Natural Sciences* (Springer, New York, 1985).
[15] R. Graham and T. Tel, Existence of a Potential for Dissipative Dynamical Systems, Phys. Rev. Lett. **52**, 9 (1984).
[16] F. Zhang, L. Xu, K. Zhang, E. Wang, and J. Wang, The potential and flux landscape theory of evolution, J. Chem. Phys. **137**, 065102 (2012).
[17] X. Fang, K. Kruse, T. Lu, and J. Wang, Nonequilibrium physics in biology, Rev. Mod. Phys. **91**, 045004 (2019).
[18] J. Wang, L. Xu, and E. Wang, Potential landscape and flux framework of nonequilibrium networks: Robustness, dissipation, and coherence of biochemical oscillations, Proc. Natl. Acad. Sci. USA **105**, 12271 (2008).
[19] J. Schnakenberg, Network theory of microscopic and macroscopic behavior of master equation systems, Rev. Mod. Phys. **48**, 571 (1976).
[20] U. Seifert, Entropy Production along a Stochastic Trajectory and an Integral Fluctuation Theorem, Phys. Rev. Lett. **95**, 040602 (2005).
[21] T. Tomé and M. J. de Oliveira, Entropy production in irreversible systems described by a Fokker-Planck equation, Phys. Rev. E **82**, 021120 (2010).
[22] H. Qian and E. L. Elson, Fluorescence correlation spectroscopy with high-order and dual-color correlation to probe nonequilibrium steady states, Proc. Natl. Acad. Sci. USA **101**, 2828 (2004).
[23] K. El Houssaini, A. I. Ivanov, C. Bernard, and V. K. Jirsa, Seizures, refractory status epilepticus, and depolarization block as endogenous brain activities, Phys. Rev. E **91**, 010701(R) (2015).
[24] J. L. Hindmarsh and R. M. Rose, A model of neuronal bursting using three coupled first order differential equations, Proc. R. Soc. London, Ser. B **221**, 87 (1984).
[25] R. FitzHugh, Impulses and physiological states in theoretical models of nerve membrane, Biophys. J. **1**, 445 (1961).
[26] D. Roy, A. Ghosh, and V. K. Jirsa, Phase description of spiking neuron networks with global electric and synaptic coupling, Phys. Rev. E **83**, 051909 (2011).
[27] C. Morris and H. Lecar, Voltage oscillations in the barnacle giant muscle fiber, Biophys. J. **35**, 193 (1981).
[28] Y. Kuznetsov, *Elements of Applied Bifurcation Theory.* (Springer, New York, 1998).
[29] A. Burrello, K. Schindler, L. Benini, and A. Rahimi, Hyperdimensional computing with local binary patterns: One-shot learning of seizure onset and identification of ictogenic brain regions using short-time iEEG recordings, IEEE Trans. Biomed. Eng. **67**, 601 (2019).
[30] F. Zhang, L. Xu, and J. Wang, The dynamic and thermodynamic origin of dissipative chaos: chemical Lorenz system, Phys. Chem. Chem. Phys. **22**, 27896 (2020).